3D integrated high gain rectenna in package with metamaterial superstrates for high efficiency wireless power transfer applications

Woosol Lee, Hae-in Kim, Sunghyun Hwang, Saeyoung Jeon, Hyunho Cho and Yong-Kyu Yoon
Department of Electrical and Computer Engineering
University of Florida
Gainesville, FL, USA
leewoosol@ufl.edu, ykyoon@ece.ufl.edu

***Abstract*— This paper first presents a 3D integrated high gain rectenna in package with metamaterial (MTM) superstrates for a high efficiency wireless power transfer (WPT) application which operates at 2.45 GHz. The integrated rectenna is composed of 3 layers where the first layer is an MTM superstrate consisting of 4 by 4 MTM unit cells (the size of the unit cell: 27.5 × 27.5 mm^2), the second layer a patch antenna (36.1 × 27.9 mm^2), and the third layer a rectifier (54.2 × 16.3 mm^2). By integrating the MTM superstrate on top of the patch antenna, the gain of the antenna is enhanced due to its focusing capability, resulting in the increase of incident RF power at the rectifier input thereby inducing high output DC power and high end-to-end efficiency. A prototype 3D integrated rectenna is designed, fabricated and characterized. It shows a gain improvement of 5.8 dB compared to a counterpart patch antenna without an MTM superstrate, and a maximum RF-DC conversion efficiency of 63.5 % at an input RF power of 10.5 dBm. This results in the improvement of the RF-DC efficiency from 56.8 % to 63.5 % and the increase of the output DC power from 1.6 mW to 6.35 mW (a factor of 3.97 improvements).**

Keywords*— Metamaterial, rectenna, wireless power transfer (WPT), gain, power transfer efficiency (PTE), rectenna in package

I. INTRODUCTION

Recently, the research and development on wireless power transfer (WPT) has been actively carried out in various areas. While near-field WPT has shown an effective means of powering commercial consumer devices, far-field WPT through radiation continues to be a highly expected solution to the power challenges related to ubiquitous sensor connectivity as envisioned in the Internet of Things (IoT). A rectenna (rectifier + antenna) is the core component of the far-field WPT system. In order to provide sufficient power to devices and sensors remotely, rectennas with a high gain antenna and a high efficiency rectifier are required. Some researchers have employed metamaterial (MTM) superstrates to enhance the gain of the antenna for signal communications [1]-[5]. MTMs are artificially engineered materials that have uncommon electromagnetic properties, such as negative refraction, thereby improving the gain of the antenna [6]. However, to the best of our knowledge, study in which MTM superstrates are integrated with a rectenna in package for WPT has not been reported.

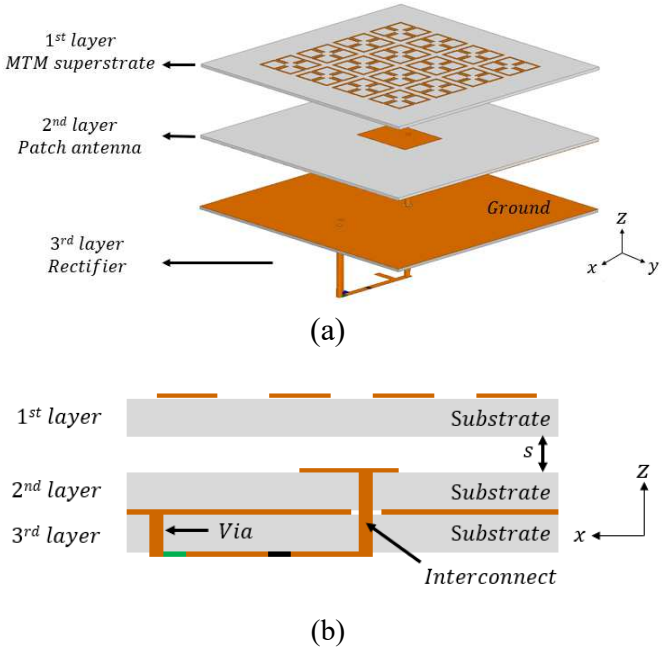

Fig. 1. Schematic of a 3D integrated rectenna: (a) perspective view, (b) side view, where $\boldsymbol{s = 10\ mm}$.

In this work, an integrated 3-layer high gain rectenna using MTM superstrates is demonstrated. The advantages of this work are as follows: 1) By integrating the MTM superstrate on top of the patch antenna, the gain of the antenna is enhanced, resulting in the increase of incident RF power at the rectifier input thereby inducing high output DC power and high end-to-end efficiency. 2) By integrating a rectifier circuit on the bottom of the antenna, which is separated by the patch antenna ground plane, the system footprint remains the same while the cross coupling between MTM superstrates and rectifiers is suppressed.

As a test vehicle, a 2.45 GHz 3D integrated rectenna which has the first layer of a superstrate consisting of 4 by 4 MTM unit

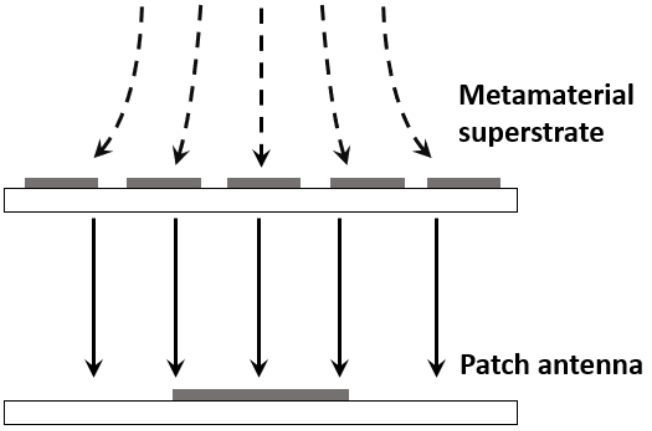

Fig. 2. Conceptual principle of gain improvement in a patch antenna using an MTM superstrate.

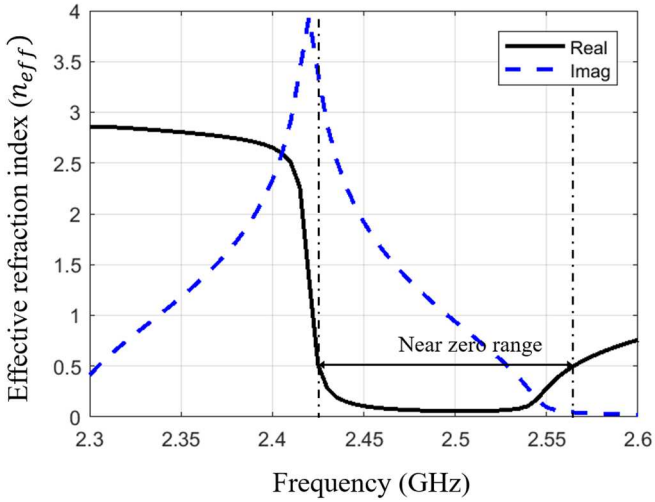

Fig. 4. Simulated effective refraction index of the MTM unit cell.

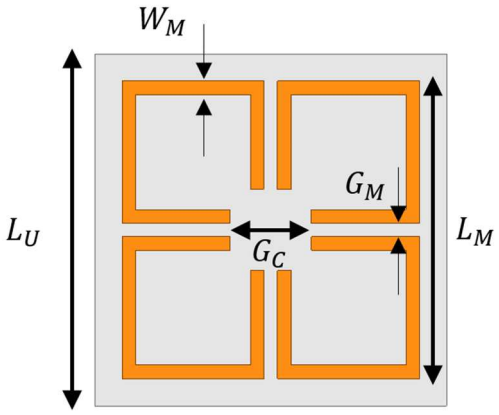

Fig. 3. Top view of the MTM unit cell, where $\boldsymbol{L_U = 27.5\ mm}$, $\boldsymbol{L_M = 23.5\ mm, W_M = 1\ mm, G_M = 1\ mm, G_C = 6\ mm}$.

cells (the size of the unit cell: 27.5 × 27.5 mm^2), the second layer of a patch antenna (36.1 × 27.9 mm^2), and the third layer of a rectifier (54.2 × 16.3 mm^2) is implemented on a three-FR4 substrate stack with a dielectric constant of 4.4, a loss tangent of 0.02, and a thickness of 1.57 mm for FR4, as shown in Fig. 1. High Frequency Structure Simulator (HFSS, Ansys Inc.) is utilized to simulate the full 3D structure of the MTM superstrate integrated antenna.

II. Design and Analysis of the 3D Integrated High Gain Rectenna

A. Design of the Metamaterial Unit Cell

First, the MTM unit cell is designed to have a zero refractive index for a high gain antenna at 2.45 GHz. Fig. 2. shows the conceptual principle of gain improvement in a patch antenna using an MTM superstrate. The MTM superstrate can change the direction of electromagnetic field at the boundary due to its refractive index near zero, thereby enhancing the gain of the antenna. In this work, a four-clover shaped MTM is utilized and the MTM unit cell is designed on a FR 4 substrate. The top view of the designed unit cell is shown in Fig. 3.

High Frequency Structure Simulator (HFSS, Ansys Inc.) is utilized to simulate the performance of a full 3D MTM unit cell. The effective refractive index can be extracted from the simulation results by using the standard retrieval methods [7]-[10]. In the simulation result (Fig. 4), the real value of η_{eff} is designed to have near zero values in the range of 2.42 to 2.56 GHz ($\eta_{eff}(re) \leq 0.5$). This means the MTM superstrate can change the direction of electromagnetic field by the boundary conditions to near zero, thereby enhancing the gain of the antenna for 2.45 GHz.

B. Design of the MTM integrated patch antenna

As shown in Fig. 1, the MTM superstrate consists of 4X4 MTM unit cells. The MTM superstrate is integrated on top of a patch antenna. The patch antenna is designed to be 36.1 mm x 27.9 mm for a 2.4 GHz BlueTooth and a WiFi application. When the MTM superstrate is placed on top of the patch antenna, it serves as the MTM lens for antenna gain improvement at 2.45 GHz.

C. Design of the Rectifier

Fig. 5 (a). shows the block diagram of the rectifier circuit. A half-wave rectifier using a HSMS2860 Schottky diode is chosen for simplicity. It also consists of a low-pass filter (200 pF shunt capacitor) and a resistive load (1k ohms). A matching circuit is used at the diode input port to ensure the maximal power transfer to the diode. As the input impedance of the proposed antenna is 50 ohms, the rectifier circuit is designed to be 50 ohms matched. The design and simulation of the rectifier circuit has been performed using Advanced Design System (ADS) as shown in Fig. 5 (b). The Harmonic Balance simulation was performed to take into account the nonlinearity of the Schottky diode. The simulation results of the rectifier circuit will be further discussed with the measurement results in Section 4.

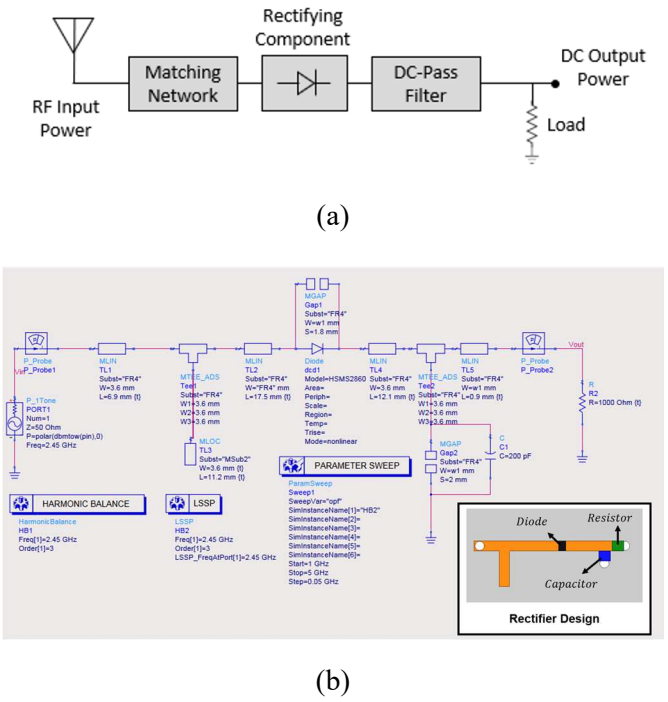

Fig. 5. (a) Block diagram of rectifier, (b) ADS schematic of the rectifier design.

TABLE I. SIMULATED PERFORMANCE OF THE PATCH ANTENNA WITHOUT AND WITH MTM SUPERSTRATE

Parameters	Without MTM superstrate	With MTM superstrate
Efficiency	97.2 %	93.9 %
Peak gain	4.78 dBi	10.7 dBi

III. FABRICATION OF THE 3D INTEGRATED HIGH GAIN RECTENNA

An FR-4 substrate has been utilized to fabricate the 3D integrated high gain rectenna on. The devices are fabricated using a milling machine. The fabricated MTM superstrate (1st layer), patch antenna (2nd layer), rectifier circuit (3rd layer), and 3D integrated rectenna are shown in Fig. 6. (a), (b), (c), and (d). The Schottky diode (HSMS 2860, Avago Technologies Inc), 1k ohms resistor (RNCP0805FTD1K00, Stackpole Electronics Inc), and 200 pF capacitor (GCM1885C2A201FA16J , Murata Electronics Inc) are utilized for the fabrication of the rectifier circuit.

IV. SIMULATED AND MEASURED RESULTS

A. *Simulated and Measured Results of the Patch Antenna without and with MTM Superstrate*

In this section, the antenna performance of the patch antenna with and without an MTM superstrate is simulated, measured, and characterized. Measurement of the return loss of the patch antennas has been carried out using a vector network analyzer

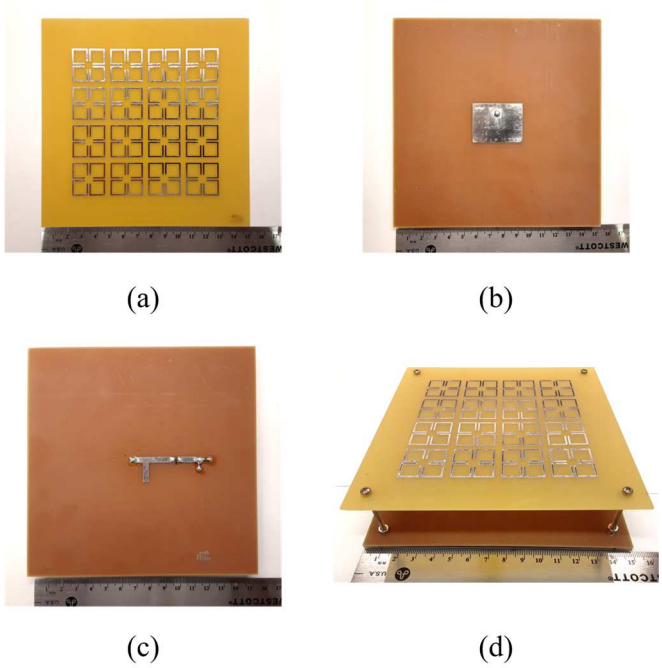

Fig. 6. (a) Fabricated MTM superstrate, (b) Fabricated patch antenna, (c) Fabricated rectifier, (d) Fabricated 3D integrated rectenna.

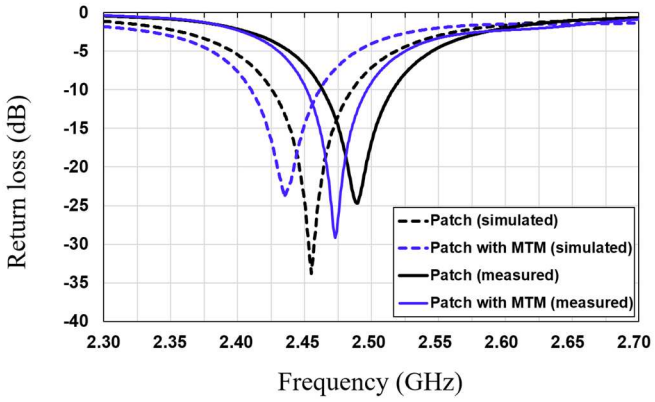

Fig. 7. Simulated and measured return loss results of the patch antenna without and with MTM superstrate.

(HP E8361A, Agilent, Inc.) after standard one port short-open-load (SOL) calibration between 2.3 GHz and 2.7 GHz. As shown in Fig. 7, the measured results of the patch without and with MTM superstrate show a return loss of 24.7 dB at 2.48 GHz and 29.1dB at 2.47 GHz, respectively, which matches well with the simulated results.

The simulated performances of the patch antenna without and with MTM superstrate are summarized in Table I. It should be noted that the peak gain of the patch antenna improves by 5.8 dB when the MTM superstrate is integrated. The resonant

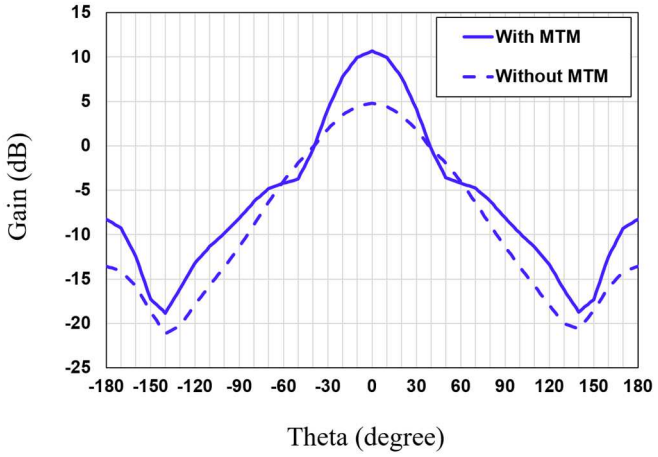

Fig. 8. Simulated radiation patterns of the patch antenna with and without MTM superstrate at 2.45 GHz.

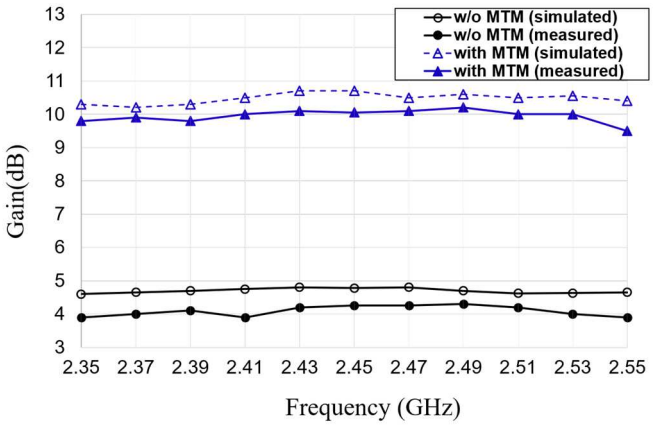

Fig. 9. Simulated and measured peak gain of the patch antenna without and with MTM.

radiation frequencies are a bit upshifted, which is attributed to fabrication tolerance, i.e. the dimension of the fabricated patch structure is reduced during fabrication. Fig. 8 shows simulated radiation patterns of the patch antenna with and without MTM superstrate at 2.45 GHz and Fig. 9 shows the simulated and measured peak gain of the antenna without and with MTM superstrate as a function of frequency. The measured gains of the antenna without and with MTM at 2.45 GHz are 4.25 dBi and 10.05 dBi, respectively. It is proved that the gain of the loop antenna is improved by 5.92 dB when the MTM superstrate is integrated on top of the patch antenna. The simulation and measurement results in this section show that the implemented MTM superstrate serves as the MTM lens and the MTM superstrate is highly effective for improving the gain of the antenna.

B. Simulated and Measured Results of the Designed Rectifier Circuit

In this section, the rectifier circuit is simulated, measured, and characterized. The simulation of the rectifier circuit has been

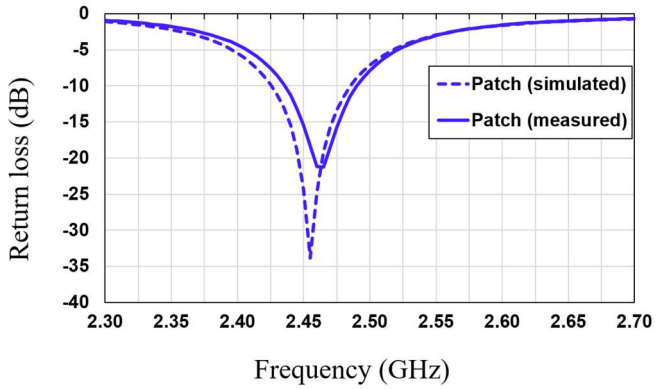

Fig. 10. Simulated and measured return loss results of the rectifier circuit.

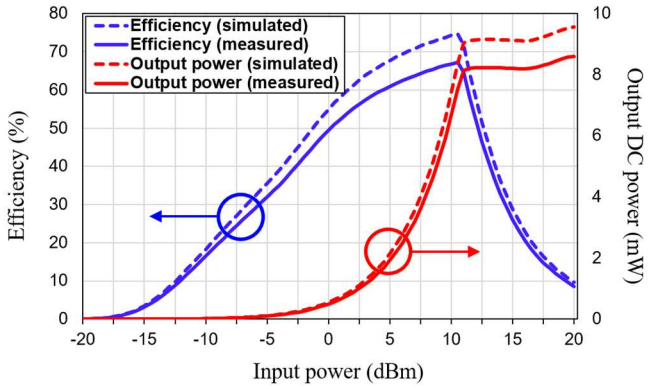

Fig. 11. Simulated and measured RF-DC conversion efficiency of the rectifier circuit.

performed using ADS and the measurement has been carried out using a vector network analyzer (HP E8361A, Agilent, Inc.), RF signal generator (HP 8648D, Agilent Inc), and multimeter (Fluke 189). First, the return loss of the rectifier circuit is simulated and measured. As shown in Fig. 10., the measured results of the rectifier circuit show a return loss of 21.3 dB at 2.47 GHz which matches well with the simulated return loss of 33.8 dB at 2.46 GHz.

In addition, the RF-DC conversion efficiency of the rectifier circuit is simulated and measured. The RF-DC conversion efficiency of the rectifier circuit can be calculated by the following equation:

$$\eta_{RF-DC} = \frac{P_{out}}{P_{in}} \times 100\ (\%) = \frac{{V_{DC}}^2}{P_{in} R_L} \times 100\ (\%) \qquad (1)$$

where P_{out} is the output DC power, P_{in} is the input RF power, R_L is the load resistance value, and V_{DC} is the output DC voltage value. The simulated and measured conversion efficiency and output DC power for 2.45 GHz at different input RF power levels are depicted in Fig. 11. A measured RF-DC conversion efficiency of 16.5 %, 49.4 %, and 67.3 % (max) are achieved at -10 dBm, 0 dBm, and 10.5 dBm, respectively. The differences

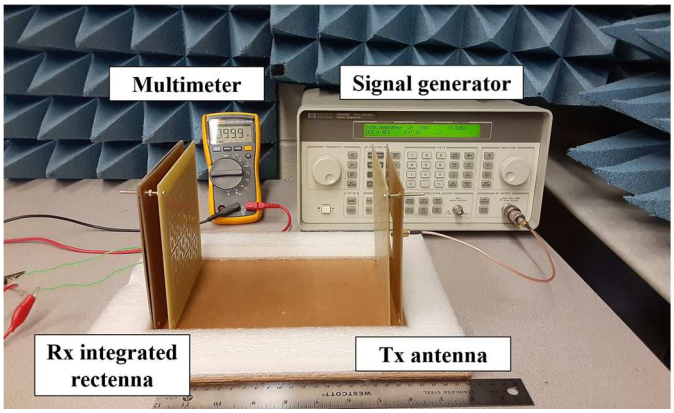

Fig. 12. Measurement setup for the proposed 3D integrated rectenna.

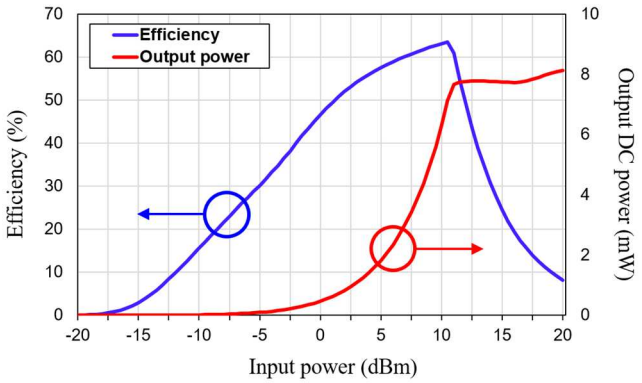

Fig. 13. Measured RF-DC conversion efficiency of the 3D integrated rectenna.

between simulated and measured results in Fig. 11 can be attributed to: 1) the insertion loss of the SMA connector between the RF signal generator and the rectifier circuit, which has not been taken into account in the ADS simulation. 2) the tolerance of the spice simulation model provided by the vendor of HSMS 2860 Schottky diode.

C. *Measured Results of the 3D Integrated High Gain Rectenna*

Finally, the 3-layer 3D rectenna is fully integrated in package with MTM superstrate. The measurement setup for the 3D integrated rectenna is shown in Fig. 12 which is composed of the RF signal generator, Tx antenna (patch with MTM), Rx integrated rectenna, and multimeter. The integrated rectenna is placed at a distance of 20 cm away from the Tx antenna. The RF-DC conversion efficiency of the rectenna can be estimated by:

$$\eta_{rectenna} = \frac{{V_L}^2}{P_r R_L} \times 100\ (\%) \qquad (2)$$

where P_r is the RF power captured by the Rx integrated rectenna, R_L is load resistance value, and V_L is output voltage on the load. The RF power captured by the Rx integrated rectenna, P_r, can be calculated by the Friis transmission equation [11]:

$$P_r = \left(\frac{\lambda}{4\pi r}\right)^2 G_t G_r P_t \qquad (3)$$

where λ is the wavelength of the operating frequency, r is the distance between Tx antenna and Rx rectenna, G_t and G_r is the gain of the Tx antenna and Rx antenna, respectively, and P_t is the Tx power. Based on the above analysis, the measured RF-DC conversion efficiency and output power of the 3D integrated rectenna versus input power can be obtained as depicted in Fig. 13. A measured RF-DC conversion efficiency of 15.4 %, 46.7 %, and 63.5 % (max) is achieved at -10 dBm, 0 dBm, and 10.5 dBm, respectively. Assuming the input power without MTM is 4.7 dBm, the input power can be increased to 10.5 dBm by integrating MTM. This results in the improvement of the RF-DC efficiency from 56.8 % to 63.5 % and the increase of the output DC power from 1.6 mW to 6.35 mW (a factor of 3.97 improvement).

V. Conclusion

In this work, the 3D integrated high gain rectenna in package with MTM superstrate is demonstrated. By integrating the MTM on top of the patch antenna, the gain of the antenna is enhanced by 5.8 dB, resulting in the increase of incident RF power at the rectifier input thereby inducing high output DC power and high end-to-end efficiency. The measured RF-DC conversion efficiency of 15.4 %, 46.7 %, and 63.5 % (max) are achieved at -10 dBm, 0 dBm, and 10.5 dBm, respectively. The improvement of the RF-DC efficiency from 56.8 % to 63.5 % and the increase of the output DC power from 1.6 mW to 6.35 mW (a factor of 3.97 improvement) assuming the input power without MTM is 4.7 dBm.

Acknowledgment

WS Lee is a recipient of the fellowship program by the Republic of Korea Army Headquarters. RF experiment/characterization has been performed at the University of Florida.

References

[1] Z.-B. Weng, N.-B. Wang, Y.-C. Jiao, F.-S. Zhang, "A directive patch antenna with metamaterial structure." *Microw. Opt. Technol. Lett. 49(2)*, 456–459, 2007.

[2] A. K. Singh, M. P. Abegaonkar and S. K. Koul, "High-Gain and High-Aperture-Efficiency Cavity Resonator Antenna Using Metamaterial Superstrate," *IEEE Antennas and Wireless Propagation Letters*, vol. 16, pp. 2388-2391, 2017.

[3] C. Kim, K. Lee, S. Lee, K. T. Kim, and Y. Yoon, "A surface micromachined high directivity GPS patch antenna with a four-leaf clover shape metamaterial slab," *2012 IEEE 62nd Electronic Components and Technology Conference*, San Diego, CA, 2012, pp. 942-947.

[4] C. Kim, H. Ahn, D. S. Elles, M. Machado and Y. Yoon, "A high gain circular polarization antenna using metamaterial slabs," *2010 IEEE Antennas and Propagation Society International Symposium*, Toronto, ON, pp. 1-4, 2010.

[5] W. Lee, H. Kim and Y. Yoon, "Metamaterial-inspired dual-function loop antenna for wireless power transfer and wireless communications," *2020 IEEE 70th Electronic Components and Technology Conference (ECTC)*, Orlando, FL, USA, pp. 1351-1357, 2020.

[6] W. J. Padilla, D. N. Basov, and D. R. Smith, "Negative refractive index metamaterials," *Mater. Today 9(7–8)*, 28–35, 2

[7] D. Smith, S. Schultz, P. Markos, and C. Soukoulis, "Determination of effective permittivity and permeability of metamaterials from reflection

and transmission coefficients," *Phys. Rev. B, Condens. Matter*, vol. 65, no. 19, 2002, Art. no. 195104.

[8] D. Smith, D. Vier, T. Koschny, and C. Soukoulis, "Electromagnetic parameter retrieval from inhomogeneous metamaterials*," Phys. Rev. E, Stat. Phys. Plasmas Fluids Relat. Interdiscip. Top.*, vol. 71, no. 3, 2005, Art. rno. 036617.

[9] X. Chen, T. M. Grzegorczyk, B.-I. Wu, J. Pacheco Jr, and J. A. Kong, "Robust method to retrieve the constitutive effective parameters of metamaterials," *Phys. Rev. E, Stat. Phys. Plasmas Fluids Relat. Interdiscip. Top.*, vol. 70, no. 1, 2004, Art. no. 016608.

[10] Z. Szabó, G. Park, R. Hedge, and E. Li, "A Unique Extraction of Metamaterial Parameters Based on Kramers–Kronig Relationship," *IEEE Transactions on Microwave Theory and Techniques*, vol. 58, no. 10, pp. 2646-2653, Oct. 2010.

[11] Y. Liu, K. Huang, Y. Yang and B. Zhang, "A Low-Profile Lightweight Circularly Polarized Rectenna Array Based on Coplanar Waveguide," *IEEE Antennas and Wireless Propagation Letters*, vol. 17, no. 9, pp. 1659-1663, Sept. 2018.